



This is a repository copy of *Estimation of seismic response parameters and capacity of irregular tunnel-form buildings*.

White Rose Research Online URL for this paper:
<http://eprints.whiterose.ac.uk/148600/>

Version: Accepted Version

Article:

Mohsenian, V., Nikkhoo, A. and Hajirasouliha, I. orcid.org/0000-0003-2597-8200 (2019)
Estimation of seismic response parameters and capacity of irregular tunnel-form buildings.
Bulletin of Earthquake Engineering. ISSN 1570-761X

<https://doi.org/10.1007/s10518-019-00679-0>

This is a post-peer-review, pre-copyedit version of an article published in Bulletin of Earthquake Engineering. The final authenticated version is available online at:
<http://dx.doi.org/10.1007/s10518-019-00679-0>

Reuse

Items deposited in White Rose Research Online are protected by copyright, with all rights reserved unless indicated otherwise. They may be downloaded and/or printed for private study, or other acts as permitted by national copyright laws. The publisher or other rights holders may allow further reproduction and re-use of the full text version. This is indicated by the licence information on the White Rose Research Online record for the item.

Takedown

If you consider content in White Rose Research Online to be in breach of UK law, please notify us by emailing eprints@whiterose.ac.uk including the URL of the record and the reason for the withdrawal request.



eprints@whiterose.ac.uk
<https://eprints.whiterose.ac.uk/>

Estimation of Seismic Response Parameters and Capacity of Irregular Tunnel-Form Buildings

Vahid Mohsenian¹, Ali Nikkhoo^{2*}, Iman Hajirasouliha³

1. Postgraduate Researcher, Department of Civil Engineering, University of Science and Culture, Tehran, Iran.
2. Associate Professor, Department of Civil Engineering, University of Science and Culture, Tehran, Iran.
3. Associate Professor, Department of Civil and Structural Engineering, University of Sheffield, Sheffield, UK.

*** Corresponding author**

Associate Professor,
Department of Civil Engineering,
University of Science and Culture, Tehran, IRAN.
Tel and Fax: +98 2142863000
Email: nikkhoo@usc.ac.ir

1 **Abstract**

2 Insufficient information about the seismic performance of tunnel-form buildings and limited
3 relevant design codes and standards are the main barriers towards application of these systems in
4 seismically active areas. Vertical and horizontal irregularity of typical tunnel-form buildings is
5 another cumbersome challenge restricting the application of these systems. To address these
6 issues, this study aims to evaluate the seismic behaviour of tunnel-form buildings with horizontal
7 irregularity and develop appropriate design methodologies. Based on the results of 3, 5, 7 and 10-
8 storey buildings, new response modification factors are proposed as a function of seismic demand
9 and expected performance level. Fragility curves are also derived for various levels of intensity,
10 and simple equations are introduced to estimate uncoupled frequency ratios. The results, in
11 general, demonstrate the flexible torsional behaviour of irregular tunnel-form structures and their
12 adequate seismic resistance capacity. The buildings studied herein, managed to satisfy the
13 Immediate Occupancy (IO) performance requirements under design-basis earthquake, which
14 implies that the plan regularity requirement for tunnel-form buildings in seismic codes may be
15 too conservative. Moreover, it is concluded that using response modification factor equal to 5 can
16 generally result in sufficient stability and adequate performance level under both design basis and
17 maximum considered earthquake scenarios.

18

19 **Keywords:** Tunnel-Form Structural System, Irregularity, Response Modification Factor,
20 Fragility Analysis, Uncoupled Frequencies Ratio.

21 **Introduction**

22 The modern construction industry is quickly moving towards more efficient structural systems
23 and technologies to reduce costs, constructional time and human resources, and also to promote
24 the quality and safety of the structures under extreme loading events such as strong earthquakes.
25 In this respect, the newly-developed tunnel-form structural systems can offer several advantages
26 such as competent capability for planning, shortening the construction time and consequently
27 leading to a rapid asset return. In the tunnel-form structures, slab and wall elements are employed
28 as the main lateral and vertical load-carrying systems, and the beam and column elements
29 commonly used in typical structural systems are excluded. Moreover, since the walls and slabs

30 are simultaneously constructed in each storey, there is no need to use cold joints to ensure an
31 integrated 3D performance of the system during a seismic event. The considerable length of wall
32 elements in this system, helps to prevent stress concentrations at wall to slab connections, which
33 are usually observed in common beam-column systems. In addition, tunnel-form structures
34 generally can provide a good level of resilient under extreme load conditions. This is confirmed
35 by the observations from Kocaeli ($M_w=7.4$) and Duzce ($M_w=7.2$) earthquakes, where most
36 tunnel-form buildings managed to withstand the strong earthquake excitations and generally
37 performed better than other commonly used RC systems (Balkaya and Kalkan 2004a).

38 Due to the above mentioned advantages, this type of structural system is increasingly become
39 popular especially for mass construction projects in seismically active areas. Despite extensive
40 use of these structures, the available codes and standards do not consider them as independent
41 structural systems. Moreover, very limited studies have been conducted to investigate the seismic
42 performance of these systems. In the following, some of the most notable studies including their
43 outcomes are briefly presented.

44 Previous studies on the behaviour of tunnel-form buildings, have demonstrated that the empirical
45 equations for calculation of fundamental period in current design guidelines, do not generally
46 yield to accurate predictions. This can result in improper estimation of the earthquake-induced
47 loads for tunnel-form buildings (Goel and Chopra 1998; Lee et al. 2000). To address this issue,
48 through a number of eigenvalue analyses on reinforced concrete (RC) buildings with different
49 plans and number of storeys, Balkaya and Kalkan (2003a) proposed a new equation to acceptably
50 estimate the fundamental period of tunnel-form buildings. Based on the outcomes of their
51 analyses, in most cases, torsional modes were precedent to the translational ones. Due to the
52 complexity and limitations of their proposed relationship, in a follow-up study they attempted to
53 develop another equation which was direction-independent (Balkaya and Kalkan 2004a).

54 In another relevant study, Balkaya and Kalkan (2003b; 2004b) carried out pushover analysis on 2
55 and 5-storey tunnel-form buildings with the same plan and found the 3D membrane action as the
56 dominant mechanism for tunnel-form buildings. They concluded that the 3D coupled tension-
57 compression performance, plays an important role in load-carrying capacity of these systems.
58 Moreover, the structures analyzed in their research, managed to meet the requirements of the
59 Turkish Seismic Design Code at the performance level of immediate occupancy (IO). Based on

60 the analytical results, they proposed to utilize response modification factor (R) of 5 and 4 for
61 shorter and taller tunnel-form buildings, respectively.

62 To investigate the nonlinear seismic behaviour of tunnel-form buildings, Tavafoghi and Eshghi
63 (2005) carried out studies on two 1-5 scale specimens. During the cyclic lateral loading process, a
64 brittle behaviour was observed. The structural damages were mainly developed in the slabs as
65 well as the slab to wall and wall to foundation connections. The forced vibration tests also
66 indicated that the cracks developed in the slabs clearly affected the period of the first vibration
67 mode. Based on their findings, the response modification factor of 4 was suggested to be a
68 reasonable value for these systems.

69 Yuksel and Kalkan (2007) carried out a number of experimental tests on intersecting walls under
70 lateral cyclic pseudo-static loads at both principal directions. Although their tested specimens had
71 minimum percentage of longitudinal reinforcement, they exhibited a brittle shear failure.
72 Subsequently, a verification study was performed to analyse models with different percentage of
73 longitudinal bars. The results demonstrated that increasing the longitudinal bars concentrated at
74 the corner of walls, has positive effects on their seismic performance. In another study, Tavafoghi
75 and Eshghi (2008) investigated the seismic behaviour of tunnel-form concrete building structures
76 with different plans and heights. It was concluded that the fundamental period of these systems in
77 each direction is directly dependent on the total height and the aspect ratio, while number of
78 storeys does not considerably affect the results. Furthermore, the first three modes of vibration
79 were reported to be independent of the height and number of walls in plan.

80 In another relevant study, Balkaya et al. (2012) investigated the effect of soil-structure interaction
81 on the mechanical characteristics of the tunnel-form structures with different geometries making
82 use of eigenvalue analysis. According to the results, several relations for calculation of the
83 fundamental vibration period of these structures were developed by taking the effect of the soil-
84 structure interaction into account. Through a case study on a 12-storey building with tunnel-form
85 system in Croatia, Klasanovic et al. (2014) demonstrated that while the structure is in the linear
86 domain, the measured fundamental period of is close to the period obtained from EC8.

87 In a more recent study, Beheshti-aval et al. (2018) evaluated the seismic performance of tunnel-
88 form system subjected to a set of near and far-field earthquake records including forward
89 directivity effects. It was shown that the forward directivity can influence the failure modes of

90 tall tunnel-form structures and reduce the reliability of the design. Mohsenian and Mortezaei
91 (2018a) also evaluated the seismic reliability of tunnel-form structures subjected to accidental
92 torsions. According to their results, eccentricity of mass centre by up to 10% of the plan
93 dimension does not considerably affect the performance of these systems. In a follow-up study,
94 Mohsenian and Mortezaei (2018b) proposed to replace the concrete coupling beam by a
95 replaceable steel beam so that the damages could be optimally distributed in plan and height of
96 tunnel-form buildings.

97 **Problem Definition and Research Novelty**

98 Due to the special construction process of tunnel-form buildings and obligation to provide
99 sufficient space to take the formworks out of the perimeter sides of the building, it is not
100 generally possible to construct structural walls in these areas. This can lead to reduction in
101 torsional stiffness of the typical tunnel-form buildings and make them susceptible to exhibit a soft
102 torsional behaviour. As discussed in the previous section, the results of the eigenvalue analysis on
103 several buildings using tunnel-form systems, imply that the torsional modes can occur at
104 frequencies lower than the translational ones, which indicates a flexible torsional behaviour. To
105 control this undesirable response, current design standards generally suggest using regular and
106 symmetric plans, which is followed by architectural limitations. Therefore, the above mentioned
107 studies on tunnel-form structural system have been mainly focused on estimation of the
108 fundamental period and evaluation of the seismic behaviour and design parameters of
109 horizontally regular buildings. Moreover, currently there is no agreement on behaviour factors
110 suitable for seismic design of tunnel-form buildings. Due to the lack of information, in most
111 seismic design guidelines the tunnel-form structural system is categorised as a subcategory of
112 load-bearing wall structural system. However, due to the interaction between well and slab
113 elements, the seismic performance of tunnel-form buildings can be completely different with
114 conventional load-bearing wall systems.

115 To bridge the above mentioned knowledge gaps in this area, this study aims to investigate the
116 seismic performance and reliability of irregular tunnel-form building by using 3, 5, 7 and 10-
117 storey structures subjected to design earthquakes with different intensity levels simultaneously
118 applied in the two principal directions. A novel approach is also utilized to develop multi-level
119 behaviour factors on the basis of earthquake hazard level and performance limit. The proposed

120 behaviour factors can be efficiently used for performance-based design (PBD) of these systems to
121 achieve specific performance targets. Finally, the reliability studies and fragility curves
122 developed using different damage measures should provide useful insight into the nonlinear shear
123 behaviour and seismic reliability of tunnel-form building structures as a new class of structural
124 systems.

125 **Methodology**

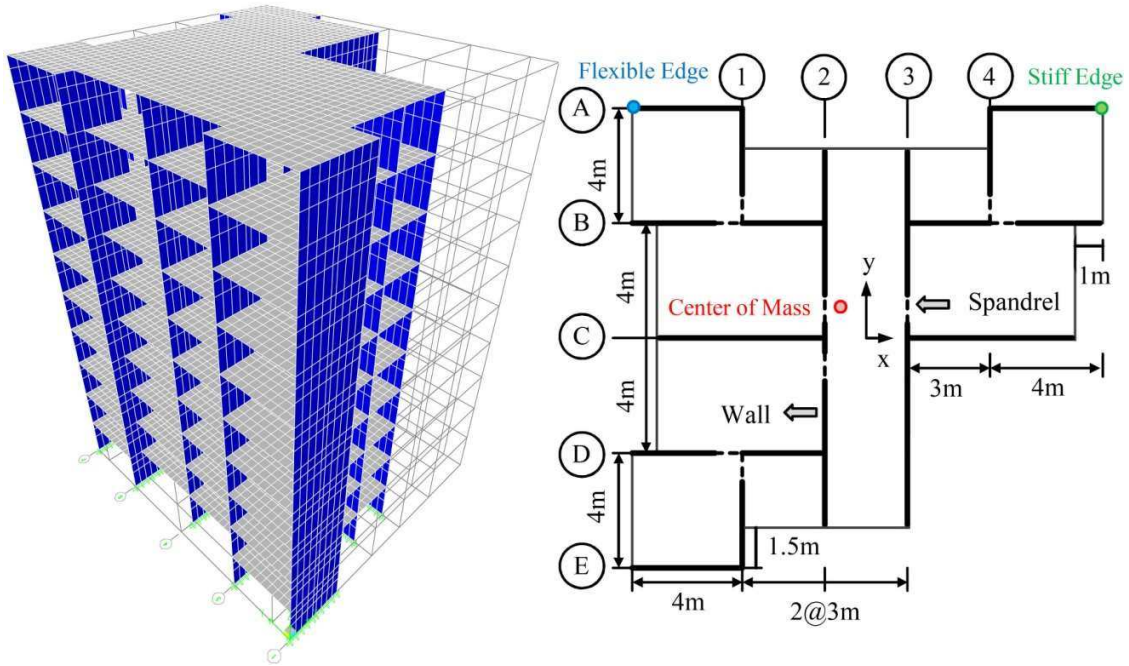
126 ○ *Specifications of numerical models*

127 In this study, the seismic performance of 3, 5, 7 and 10-storey tunnel-form buildings is
128 investigated. Fig. 1 shows the general plan view of the studied buildings as well as the 3D View
129 of the 10-Storey Model. The dotted lines in this figure represent coupling beams with length and
130 height equal to 1 and 0.7 m, respectively. The storey heights are considered to be 3 m. The
131 buildings are assumed to be in high seismic zones with soil type “II” (the shear wave velocity
132 ranges from 375 to 750 m/s) according to ASCE-07 (2016). To ensure that the buildings are
133 irregular in plan, the reentrant corners are around 40% and 50% of the plan dimension in X and Y
134 directions, respectively. It should be mentioned that similar criteria are used in the Iranian Code
135 of Practice for Seismic Design of Buildings (Standard No. 2800).

136 The buildings were designed based on ACI 318 (2014) by means of ETABS (CSI 2015)
137 Software. Besides, all the requirements prescribed by the Iranian Building and Housing Research
138 Center (BHRC 2007) for tunnel-form buildings were satisfied except the requirement for
139 horizontal and vertical regularity.

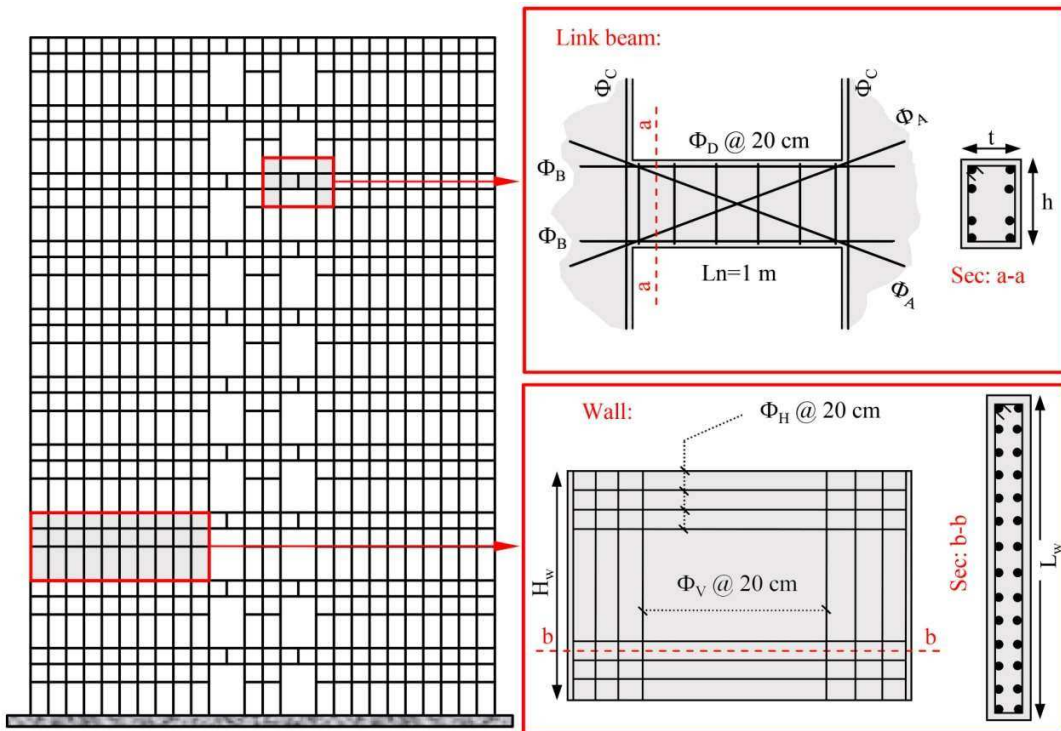
140 Fig 2 shows the schematic view of detailing and arrangement of reinforcing bars in the walls and
141 coupling beams for the 10-storey building. The thickness of the wall and slab elements was 20
142 and 15 cm, respectively. Vertical and horizontal reinforcing bars (ϕ_v and ϕ_H) were placed in two
143 layers. The longitudinal bars in the first four storeys of the 10-storey building and the first two
144 storeys of the 7-storey building had 12 mm diameter. For the rest of the elements, that diameter
145 of the longitudinal bars was 8 mm. To provide enough ductility and increase the shear strength of
146 the coupling beams (with free length to height ratio of less than 2), in addition to the special
147 transverse reinforcement (ϕ_D), diagonal reinforcement (ϕ_A) was also utilized as suggested by
148 Paulay and Binney (1974) and Zhao et al. (2004). The compressive strength of concrete material
149 and yield strength of steel bars were 25 and 400 MPa, respectively.

150



151
152
153

Fig (1): Plan view of the studied tunnel-form buildings and 3D view of the 10-storey model

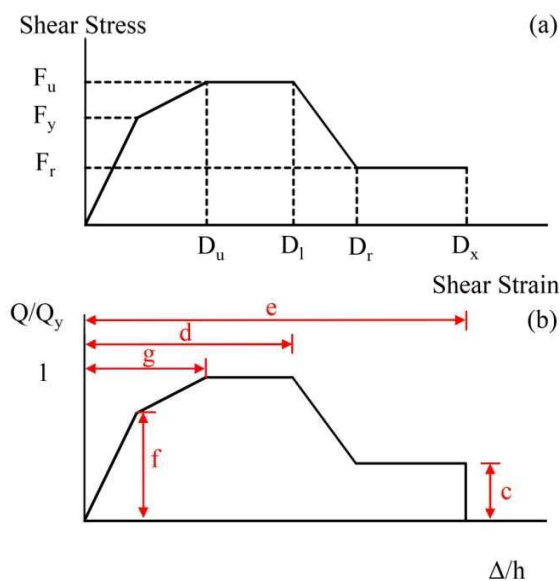


154
155
156

Fig (2): Schematic representation of detailing and arrangement of reinforcing bars in the walls and coupling beams

157 ○ *Nonlinear modelling and determination of strength and deformation parameters*

158 In this study, PERFORM-3D (CSI 2016) Software was utilized to carry out nonlinear analyses on
 159 the designed tunnel-form structures. Since the walls and coupling beams were modelled by using
 160 “Shear Wall” elements, the shear strain has been adopted as the deformation-controlled parameter
 161 for these elements (Allouzi and Alkloub 2017). Fig (3) shows the nonlinear shear behaviour
 162 defined for walls and coupling beams. The parameters required for modelling as well as their
 163 acceptance criteria were specified in accordance with the general load-displacement relation
 164 developed for the shear-control concrete elements prescribed by ASCE14-13 (2014).



165

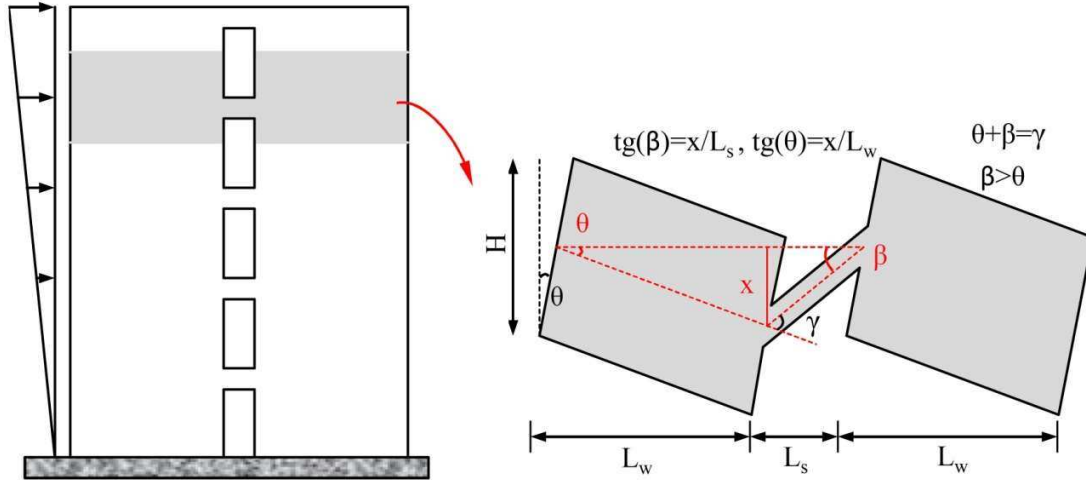
166

167 **Fig (3): Nonlinear shear behaviour of walls and spandrels (a) adopted in the software, and (b) proposed in**
 168 **ASCE41-13 (2014) for the shear control members**

169 In case of walls and shear-control beams, in which ductility is mobilized by means of shear
 170 failure, drifts (θ) and chord rotation (γ) were used as the main performance response criteria in
 171 accordance with ASCE14-13 (2014). Fig. 4 shows the schematic view of the selected
 172 deformation control parameters. It should be noted that the other internal actions in these
 173 elements (i.e. axial force and bending moment) are considered as force-control parameters.

174 Nominal shear strength was considered for modelling the nonlinear shear behaviour of elements.
 175 It should be mentioned that the relations used for deep beams, were applied to calculate the
 176 nominal strength of the coupling beams due to their notable length to height ratio (Paulay and
 177 Binney 1974; Zhao et al. 2004). The slabs were modelled as rigid diaphragms using shell

178 elements. The walls were assumed to have rigid connections at their base, while the foundation
 179 uplift was neglected.



180
 181 **Fig (4): Introduction of the deformation parameters (θ and γ)**
 182
 183

184 ○ **Nonlinear Analyses**

185 The assumptions made for gravity loading in the preliminary design phase were also considered
 186 for nonlinear analyses. The upper limit of gravity load effects was accounted for the gravity and
 187 lateral load combination based on Equation (1) as recommended by ASCE 41-13 (2014):

$$Q_G = 1.1[Q_D + Q_L] \quad (1)$$

188 where Q_D and Q_L denote the dead and effective live loads, respectively.

189 Considering the position of mass centre and centre of rigidity as well as the percentage of walls
 190 distributed in the plan, it is found that stiffness and strength of structures and eccentricity of the
 191 mass in proportion to the centre of rigidity, is greater in longitudinal (x) compared to the
 192 transverse (y) direction. On this basis, the transverse direction was considered as the principal
 193 direction of the structures.

194 The results of eigenvalue analysis on the 3, 5, 7 and 10-storey designed buildings are given in
 195 Table (1). The values of the coefficient of translational effective mass in longitudinal and
 196 transverse directions (x and y, respectively) indicate the flexible torsional behaviour of the
 197 models. It can be also seen that translational and torsional displacements are coupled in the first
 198 vibration mode.

199

Table (1): Vibration period (T) and coefficient of translational effective mass factor (M)

Mode No.	3-Storey			5-Storey		
	T(sec)	Mx (%)	My (%)	T(sec)	Mx (%)	My (%)
1	0.1067	0	10.6	0.2352	0	7.5
2	0.0693	21.2	54.3	0.1431	7.5	65
3	0.0636	52	27.0	0.1182	66.3	7.2
4	0.0285	0	3.06	0.0550	5.6	15.3

200

Mode No.	7-Storey			10-Storey		
	T(sec)	Mx (%)	My (%)	T(sec)	Mx (%)	My (%)
1	0.4153	0	6.1	0.7833	0	5.2
2	0.2450	3.9	66.3	0.4524	2.3	69
3	0.1822	66.4	4.0	0.2971	65	2.3
4	0.0895	4.1	10.8	0.1564	2.4	13

Mx → Effective translational mass factor in “x” direction.

My → Effective translational mass factor in “y” direction.

201 In the following section, the performance level of the selected tunnel-form buildings is evaluated
 202 subjected to the design basis earthquake (DBE) and maximum considered earthquake (MCE)
 203 hazard levels using fragility and incremental dynamic analysis (IDA). It is of note that all models
 204 were simultaneously excited in both principal directions. In nonlinear dynamic analyses, the
 205 second-order effects (i.e. P- Δ) were taken into account and the Rayleigh damping model with a
 206 constant damping ratio of 0.05 was assigned to the models.

207 Incremental Dynamic Analysis (IDA)

208 Incremental dynamic analysis (IDA) is a computational analysis method in which the concept of
 209 scaling ground motion records is used to estimate the demand and capacity of a structure in a
 210 wide range of behaviour from linear to failure phase (Vamvatsikos and Cornell 2002). By using a
 211 number of earthquake records in IDA, the impact of variation in the parameters related to the
 212 accelerograms (e.g. amplitude, strong-motion duration, frequency content) can be studied. The
 213 selection of appropriate earthquake records including their intensity and response parameters are
 214 considered as the main requirements of this analysis. By increasing the number of earthquake
 215 records used for IDA, the earthquake-related uncertainties are reduced; however, the
 216 computational time and volume of the outputs can significantly increase. Based on the
 217 recommendations by previous studies (e.g. Shome and Cornell 1999), using at least 10
 218 accelerograms for IDA can lead to satisfactory results. Therefore, in this study 10 pairs of
 219 earthquake records were selected from the Pacific Earthquake Engineering Research Center
 220 online database (PEER). All the selected accelerograms were far-field earthquakes recorded on

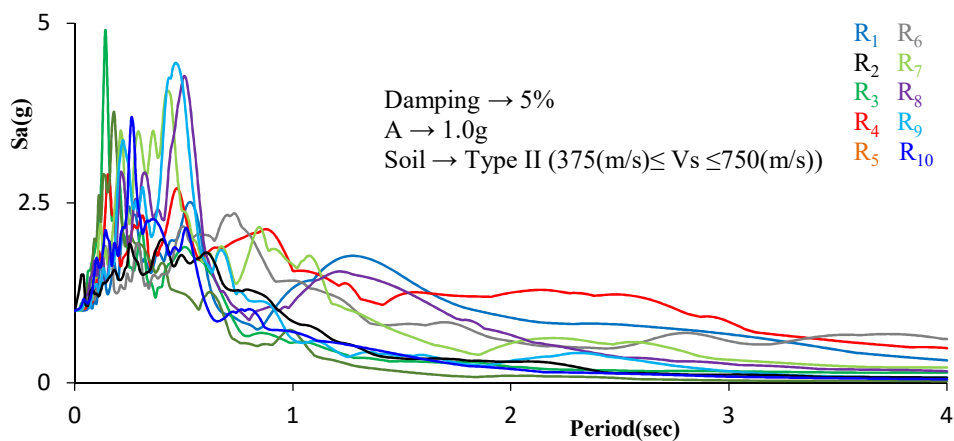
221 the sites with soil class “II” (shear wave velocity ranges from 375 to 750 m/s) in accordance with
 222 ASCE-07 (2016). Table 2 lists the characteristics of the records including their closest distance to
 223 fault rupture, magnitude and peak ground acceleration (PGA).

224 By comparison between the spectral response of each pair of accelerogram, the main component
 225 was selected based on the greater spectral values in the vibration frequency range of the
 226 structures and applied to the buildings in the “y” direction. The less intense component was
 227 simultaneously applied to the perpendicular direction (x). Fig (5) compares the acceleration
 228 response spectra of the main components of the selected records scaled to their PGA.

Table2: Selected earthquake records for time-history analysis

Record No.	Earthquake & Year	Station	R ^a (km)	Component	M _w	PGA (g)
R1	Cape Mendocino, 1992	Eureka – Myrtle & West	42	90	7.1	0.178
R2	Northridge, 1994	Hollywood – Willoughby Ave	23	180	6.7	0.246
R3	Northridge, 1994	Lake Hughes #4B - Camp Mend	33	90	6.7	0.063
R4	Cape Mendocino, 1992	Fortuna – Fortuna Blvd	20	0	7.1	0.116
R5	Northridge, 1994	Big Tujunga, Angeles Nat F	20	352	6.7	0.245
R6	Landers, 1992	Barstow	35	90	7.4	0.135
R7	San Fernando, 1971	Pasadena – CIT Athenaeum	25	90	6.6	0.110
R8	Hector Mine, 1999	Hector	12	90	7.1	0.337
R9	Kobe, 1995	Nishi-Akashi	9	0	6.9	0.509
R10	Kocaeli (Turkey), 1999	Arcelik	54	0	7.5	0.219

^a Closest Distance to Fault Rupture



229 **Fig (5): The acceleration response spectra of the selected records scaled to their PGA**
 230 The earthquake records applied to the structure were incrementally intensified within the IDA,
 231 while a similar scale factor was used for both ground motion components. Here, the intensity
 232

233 measure and the structural response to the input motion are denoted by IM and DM, respectively.
234 The fragility curves demonstrate the relation between these two parameters.

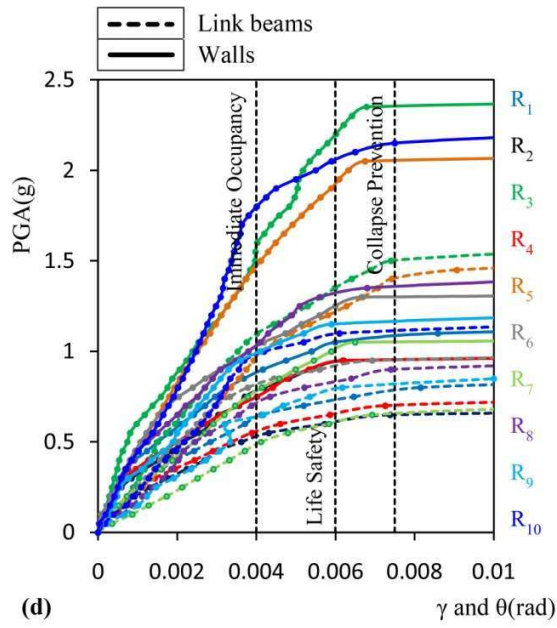
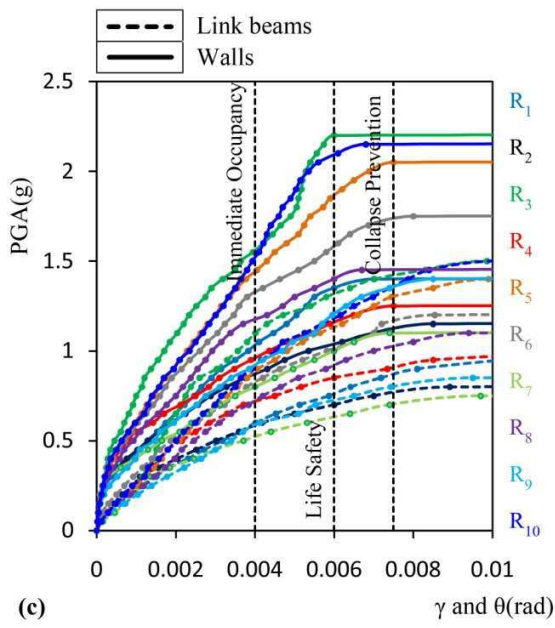
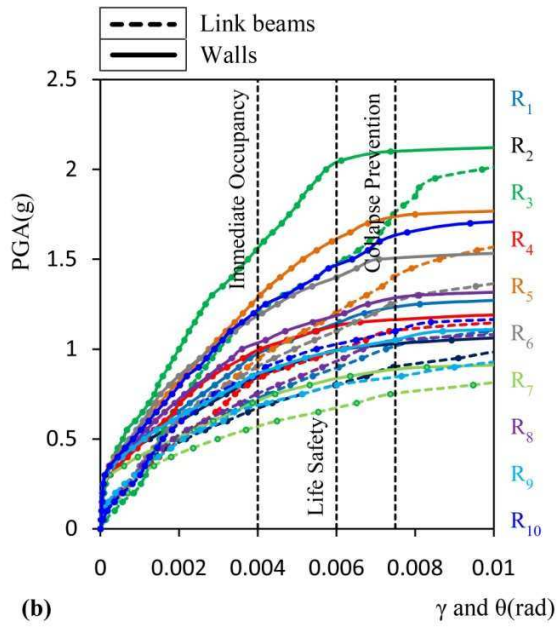
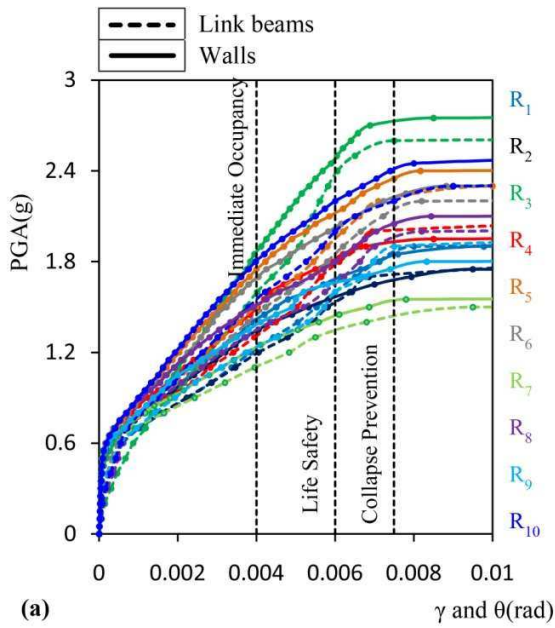
235 It should be noted that, due to the irregularity of the selected buildings, the torsional and
236 translational components of the first vibration mode are coupled in this study (see Table 1).
237 Therefore, using the spectral acceleration of the first vibration mode as the seismic intensity
238 measure would be inadequate. To address this issue, in this study the peak ground acceleration
239 (PGA) was chosen as intensity measure (IM), since it is independent of the structural
240 characteristics.

241 Different global damage indexes and particularly inter-storey drifts are generally taken as the
242 damage measure parameter (DM) in IDA. For the tunnel-form buildings studied herein, as the
243 elements are shear-control and due to lack of specific values to quantitatively define the global
244 damage indexes for this novel system, maximum drift and chord rotation developed in the walls
245 and coupling beams were adopted as the main damage parameters in IDA (see Fig (4)). It should
246 be mentioned that the global damage indexes proposed by Chobarah (2004) for squat walls could
247 be also employed, but in order to enhance the reliability on the results, the latter parameters were
248 chosen.

249 The curves obtained from the IDA analyses and the corresponding statistical percentiles are
250 illustrated in Figs (6) and (7), respectively. It is shown that, in general, the PGA level required for
251 the walls and coupling beams to reach various performance levels, is several times higher than
252 that of the DBE hazard level. Thereby, it is reasonable to expect these buildings exhibit an elastic
253 behaviour even during strong ground motions. Additionally, it can be noticed that in comparison
254 with the walls, the coupling beams reach the performance levels at lower PGA levels. As shown
255 in Fig (4), this might be attributed to the larger seismic demand of such elements. The results in
256 Figs (6) and (7) also show that the PGA level corresponding to a certain performance level, is
257 reduced for taller buildings.

258 It was found that the walls located on the axis 4 of the plan (see Fig (1)), exhibit greater seismic
259 demands and hence, these elements reach the different performance levels earlier than the other
260 walls. This is due to the fact that the torsion induced as a result of horizontal-irregularity
261 intensifies the displacement demands in the perimeter parts of the buildings.

262



263

(a)

(b)

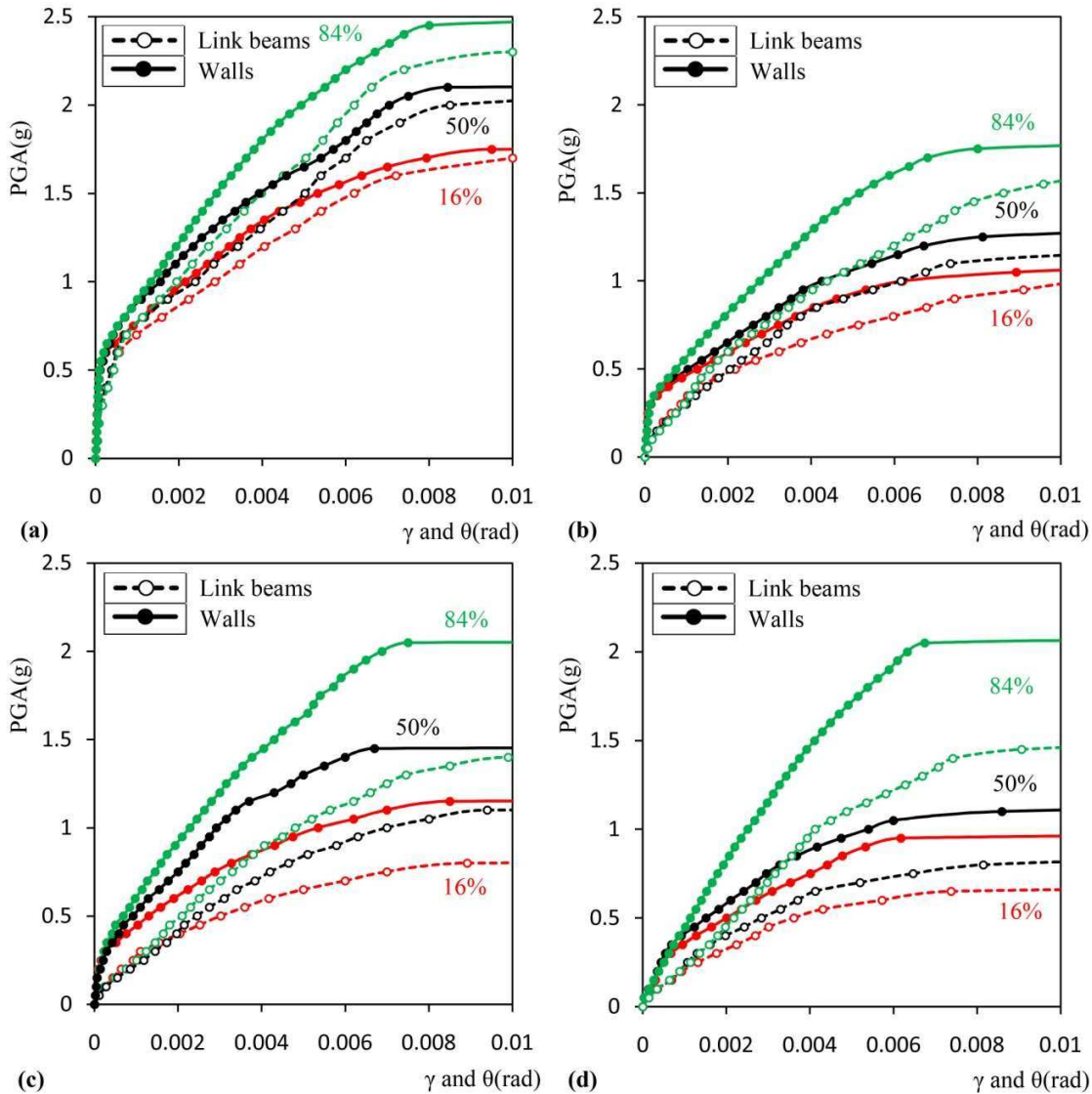
264

(c)

(d)

265 **Fig (6): Incremental Dynamic Analysis (IDA) results and the Limit States for (a) 3-storey, (b) 5-storey, (c) 7-**
 266 **storey, and (d) 10- storey buildings**

267



268

269

270

271

272

273 **Generation of Fragility Curves Using IDA**

274 Many uncertainties can affect the accuracy of the seismic performance assessment of a building
 275 under earthquake events (Hajirasouliha et al. 2016). Such uncertainties are generally classified
 276 into two groups. The first group deals with the existing uncertainties in nature such as the
 277 differences lying in the material properties, ambient effects etc. The second group concerns the
 278 uncertainties due to the errors in the computational methods, modelling procedures etc (Ang and
 279 Tang 2007; Berahman and Behnamfar 2007). In such conditions, expression of the building's

280 performance in a probabilistic form (e.g. using fragility curves) appears to be the most logical
281 approach. The fragility curves represent the cumulative distribution of loss (Cimellaro et al.
282 2006), and can be mathematically written as in Equation (2):

$$Fragility = P[R > LS_i | IM = S] \quad (2)$$

283 where, R represents the building's response, LS_i denotes the performance level or limit state
284 related to R , IM (intensity measure) is the intensity of the input earthquake ground motions, and S
285 is a particular value of IM .

286 The distribution of structural responses at different levels of earthquake intensity can be
287 demonstrated by using fragility curves. The fragility curves can be also utilized as efficient tools
288 to assess the seismic vulnerability of both structural and non-structural elements (Nielson 2005;
289 Kinali 2007). Different methods can be used to generate fragility curves including experts'
290 judgments, empirical-statistical approach, experimental, analytical and combined methods
291 (Khalvati and Hosseini 2008). In this study, the fragility curves were generated by means of
292 analytical or IDA analysis. By using the lateral drift and chord rotation as the damage measure
293 parameters for the walls and coupling beams, the performance levels defined by ASCE41-13
294 (2014) were considered as the damage criteria (see Fig (6)). Subsequently, fragility curves were
295 generated for each event of exceedance from these damage states as shown in Fig (8).

296 Table 3 lists the probability of exceeding the performance levels of Immediate Occupancy (IO),
297 Life Safety (LS) and Collapse Prevention (CP) in DBE and MCE hazard scenarios for the 3, 5, 7,
298 and 10- storey buildings. The results show the early damage in the coupling beams compared to
299 the walls, which indicates these elements can play the role of seismic fuse in tunnel-form
300 buildings. In all the buildings used in this study, the probability of exceeding the IO performance
301 level for coupling beams under DBE and MCE hazard levels was less than 2 and 19%,
302 respectively. Accordingly, these values for the walls in the event of DBE and MCE scenarios
303 were around 0 and less than 2%. Based on the results, it can be concluded that the studied tunnel-
304 form buildings can practically satisfy IO performance level even under very strong earthquake
305 events.

306

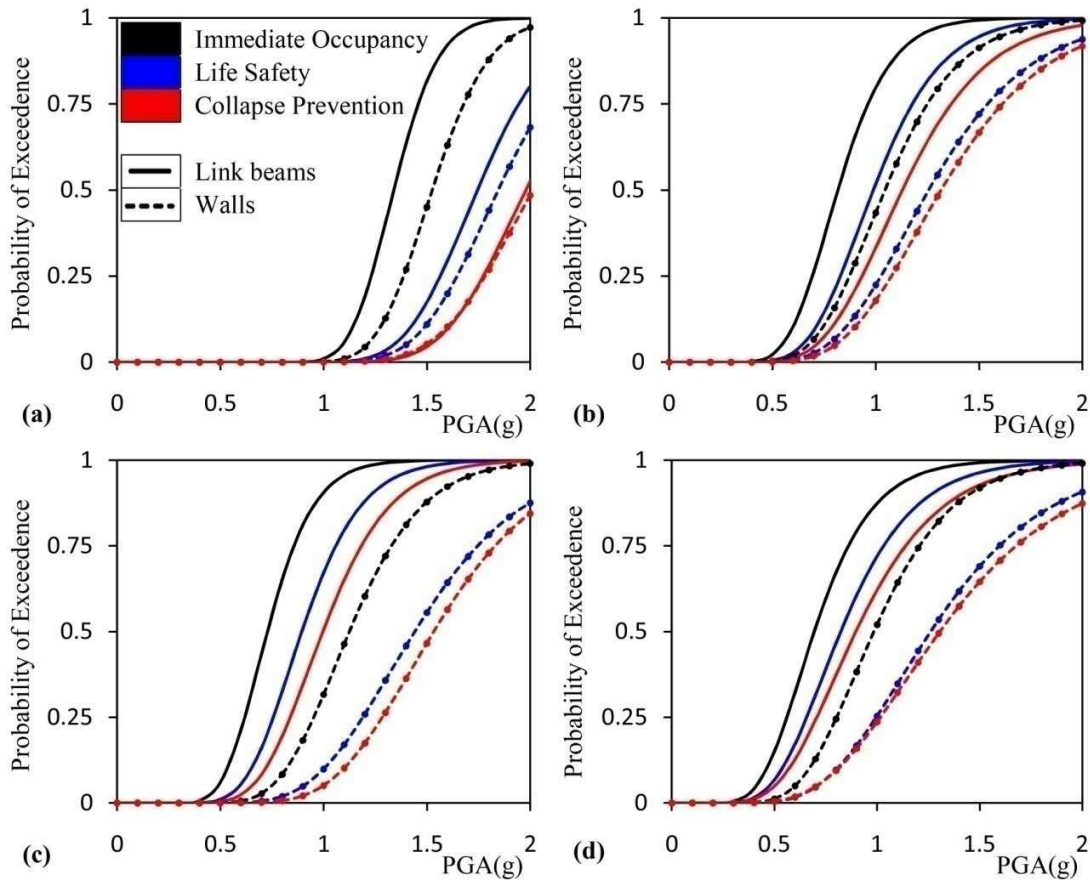
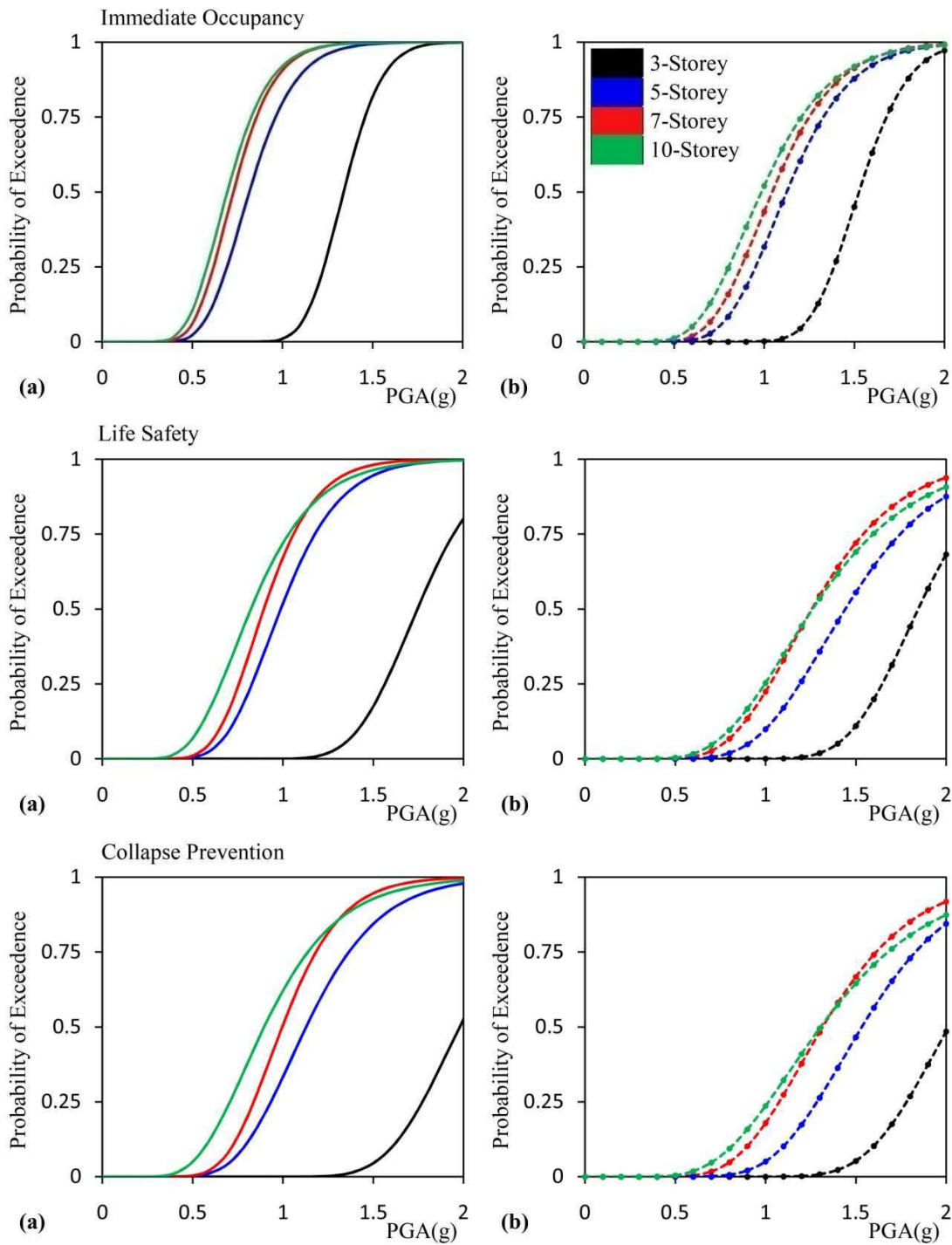


Fig (8): Fragility curves for (a) 3-storey, (b) 5-storey, (c) 7-storey, and (d) 10-storey buildings

Table (3): Probability of exceeding the performance levels of Immediate Occupancy (IO), Life Safety (LS) and Collapse Prevention (CP) in DBE and MCE hazard scenarios (%)

Hazard Levels →		Design Basis Earthquake			Maximum Considered Earthquake		
buildings	Elements	IO	LS	CP	IO	LS	CP
3-Storey	Beam	0	0	0	0	0	0
	Wall	0	0	0	0	0	0
5-Storey	Beam	0	0	0	3.43	0.75	0.33
	Wall	0	0	0	0.5	0.2	0.1
7-Storey	Beam	0.15	0	0	12.2	2.5	0.98
	Wall	0	0	0	1.83	0.6	0.58
10-Storey	Beam	1.5	0.5	0.3	18.9	8.8	6.4
	Wall	0	0	0	2.65	0.87	1

Comparison between the fragility curves depicted in Fig (9) demonstrates that, in general, by increasing the building's height, the probability to exceed various performance levels increases. This trend becomes more profound in the case of coupling beams.



321 **Fig (9): Comparison between fragility curves of the 3, 5, 7 and 10-storey buildings: (a) Link beams; (b) Walls**

322
323
324
325

326 **Estimation of Response Modification Factor**

327 ○ *Code-Based Response Modification Factor (R_{Code})*

328 The response modification factors provide by the seismic codes are mainly based on engineering
329 judgments, experiences and lessons learned from the past earthquakes. Many researchers have
330 studied the limitations of code-based response modification factors (R_{Code}), concluding that a
331 more rigorous estimation can lead to higher reliability in the methods and provisions prescribed
332 by the seismic codes (e.g. Whittaker et al. 1999). One of the problems with the response
333 modification factor introduced by seismic design codes (R_{Code}) as “force-based method” is that it
334 is unclear what level of intensity and performance can be achieved.

335 As tunnel-form structural system has recently emerged, very limited information is available
336 regarding its performance in the past earthquakes. In addition, currently in most seismic codes
337 this system is considered as a subcategory of “reinforced concrete (RC) bearing wall system”.
338 Therefore, depending on the level of ductility, the response modification factor for tunnel-form is
339 typically considered to be between 3 to 5 (e.g. BHRC 2007; Standard No.2800 2014). However,
340 considering the 3D behaviour of this structural system due to the interaction between intersecting
341 walls and floor slab, it is not very logical to adopt the parameters related to the RC bearing wall
342 with a 2D performance. This highlights the need to develop suitable behaviour factors for tunnel-
343 form buildings as discussed in the previous sections.

344 ○ *Demand-Based Response Modification Factor, R_{Demand} (Displacement/Ductility)*

345 The value of demand response modification factor depends on site seismicity as well as physical
346 and geometrical specifications of the building. Several studies have indicated that the parameters
347 like earthquake magnitude and focal depth do not considerably influence this factor compared to
348 the other parameters such as ductility, energy absorption, fundamental period, over-strength,
349 redundancy, number of degrees of freedom and soil type (Lia and Biggs 1980; Miranda 1991;
350 ATC-19 1995).

351 In this study, demand-based response modification factor, R_{Demand} , is calculated based on the
352 following equation:

$$R_{Demand} = R_{\mu}^{MDOF} \cdot \Omega_S \cdot R_d \quad (3)$$

353 where R_{μ}^{MDOF} denotes the modification factor originated from ductility and dissipated energy
354 caused by residual behaviour directly extracted from the actual structure comprising of multi
355 degrees of freedom; “ Ω_s ” represents the over-strength factor, by which the effect of redistribution
356 of actions due to redundancy is also considered; and R_d is called the allowable stress factor. It
357 should be mentioned that as the loads and resistance of materials are multiplied by safety factors
358 in allowable stress or ultimate strength design methods, it is required to utilize R_d to reduce the
359 forces to the design strength level. These parameters are calculated based on Equations (4) to (6)
360 (Fanaie and AfsarDizaj 2014).

$$R_{\mu} = V_e / V_y \quad (4)$$

$$\Omega_s = V_y / V_s \quad (5)$$

$$R_d = V_s / V_d \quad (6)$$

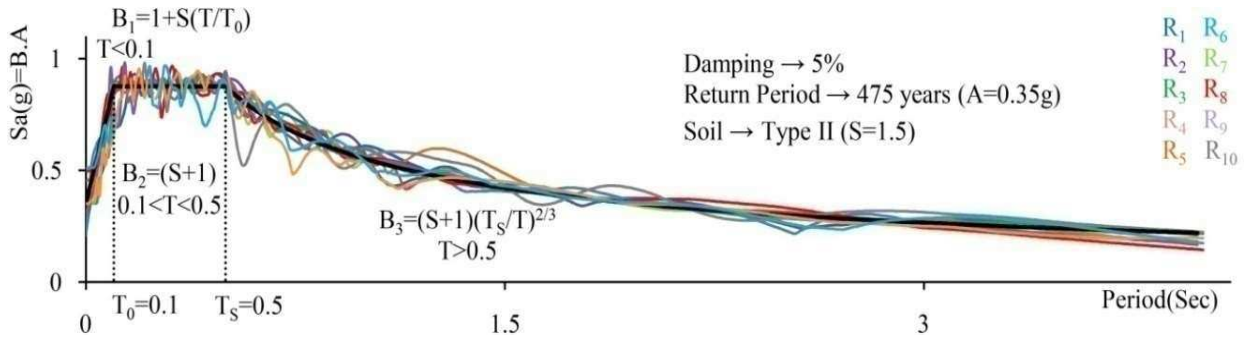
361 To attain these factors, the following parameters are introduced:

362 For a certain level of intensity, demand spectrum of the site is prepared and the earthquakes
363 compatible with this spectrum are selected. The selected earthquakes which are called demand
364 earthquakes are applied to the structure assuming a linear behaviour, and then the base shear is
365 recorded. The average of the base shear values obtained, is called elastic base shear (V_e). In this
366 study, artificial accelerograms corresponding to the code-based design spectrum were employed,
367 so that the design earthquakes could be compatible with the site hazard as much as possible. In
368 doing so, 10 artificial earthquake records were extracted based on the wavelet transform function
369 from the demand spectrum and then, applied to the structures as shown in Fig (10). It should be
370 noted that the earthquakes given in Table (2), have been utilized to produce the artificial records
371 (Hancock et al. 2006).

372 In the next step, the demand earthquakes were applied to the structure assuming a nonlinear
373 behaviour and the maximum roof displacement was obtained. Average of the drift values induced
374 by the DBE hazard scenario was taken as the target on the capacity curve. After bi-linearization
375 of this curve on the basis of ASCE41-13 (2014), yield base shear (V_y) is obtained. The shear
376 corresponding to the commencement of nonlinear behaviour (V_s), is defined as the point where
377 the capacity curves obtained based on linear and nonlinear behaviour are separated. Design base
378 shear (V_d) is calculated by dividing the linear spectral acceleration multiplied by total building’s
379 weight to the code-based response modification factor. Fig (11) shows the bi-linearization of the
380 capacity curve and the parameters used to calculate the response modification factor.

381 For the studied buildings, the demand response modification factors R_{Demand} are obtained
 382 according to the above procedure and presented in Table (4).

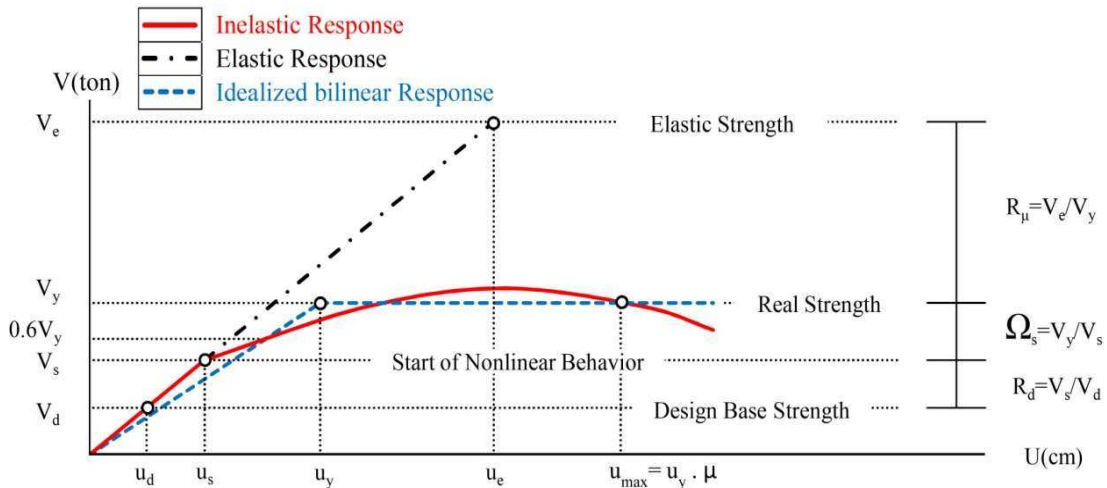
383



384

385 **Fig (10): Comparison between artificial accelerograms and site demand spectra**

386



387

388 **Fig (11): Bi-linearization of the capacity curve and introduction of parameters used to calculate the response**
 389 **modification factor**

390

Table (4): Code and Demand Response Modification Factors for the studied buildings

	R_{Code}	R_{Demand}			
		3-Storey	5-Storey	7-Storey	10-Storey
PGA(g)	0.35	0.35	0.35	0.35	0.35
Ve(ton)	--	540.1	878.5	1200.3	1559.3
Vy(ton)	--	280	465	446.8	500
Vs(ton)	--	109	220	302	400
Vd(ton)	--	132.9	228.7	324.5	468.2
Rμ	--	1.92	1.89	2.68	3.118
Ω_s	--	2.57	2.114	1.48	1.25
Rd	--	1	1	1	1
R	5	4.955	3.993	3.975	3.898

391 ○ **Supply Response Modification Factor, R_{Supply} (Capacity)**

392 This factor depends on the building's capacity to withstand nonlinear deformations to satisfy the
 393 required performance levels. The buildings can be designed based on the force-based method
 394 using a strength reduction factor assuming a certain damage level under DBE hazard scenario
 395 (Fajfar 2000). This approach is currently utilized for seismic assessment of existing buildings.
 396 The algorithm taken to derive the supply response modification factor, R_{Supply} , based on the
 397 lateral strength of structures is as follows (ATC-40 1996; Mwafy and Elnashai 2002).

398 Assuming a nonlinear behaviour for the structure, incremental dynamic analysis (IDA) is
 399 conducted on the structure making use of the earthquake records attributed to the site conditions.
 400 Subsequently, PGA factors triggering damages (in this study, reaching the structural walls to the
 401 performance level of life safety) are obtained. Afterwards, under the PGA values obtained from
 402 the previous step, linear dynamic analysis is conducted and the mean value of the resulted base
 403 shears is calculated (V_e). In the next step, by using modal lateral load distribution, a pushover
 404 analysis is performed on the structure to reach the target displacement corresponding to the
 405 damage levels obtained from the first step. By bi-linearizing the capacity curve (see Fig (11)), the
 406 yield base shear (V_y) is identified. The rest of the parameters required to calculate R_{Supply} are
 407 similar to those explained in the previous section. Table (5) shows the results of the supply
 408 response modification factor for the studied buildings.

409 **Table (5): Code and Supply Response Modification Factors for the studied buildings**

	R_{Code}	R_{Supply}			
		3-Storey	5-Storey	7-Storey	10-Storey
PGA(g)	0.35	1.88	1.56	1.46	1.23
Ve(ton)	--	1653.4	2126.2	2870.8	3599.6
Vy(ton)	--	696	630	552	500
Vs(ton)	--	109	220	302	400
Vd(ton)	--	132.9	228.7	324.5	468.2
R_{μ}	--	2.38	3.38	5.20	7.20
Ω_s	--	6.39	2.86	1.83	1.25
Rd	--	1	1	1	1
R	5	15.169	9.665	9.505	9

410
 411 As shown in Fig (12), supply response modification factors for the studied buildings based on the
 412 corresponding hazard levels, are smaller than the demand factor. This indicates the high strength
 413 of these structures to sustain intense hazard levels in highly seismic areas as discussed before. For

414 each ordered pair in (A_0) zone shown in Fig (12), walls as the main load-resisting members in
415 tunnel-form buildings remain in elastic range of behaviour. It means that for the selected DBE
416 hazard level (specified by Standard No.2800) and response modification factor of 4, the walls
417 will exhibit insignificant shear strain under this level of intensity. Selection of an R-factor
418 ranging from demand to supply values corresponding to a specific damage level, will ensure the
419 structure satisfies the desired performance level for the design intensity level. As an instance, for
420 each ordered pair in the red zone (A) shown in Fig (12), the shear strain developed in the walls
421 will be less than the limit values corresponding to the performance level of life safety (LS).

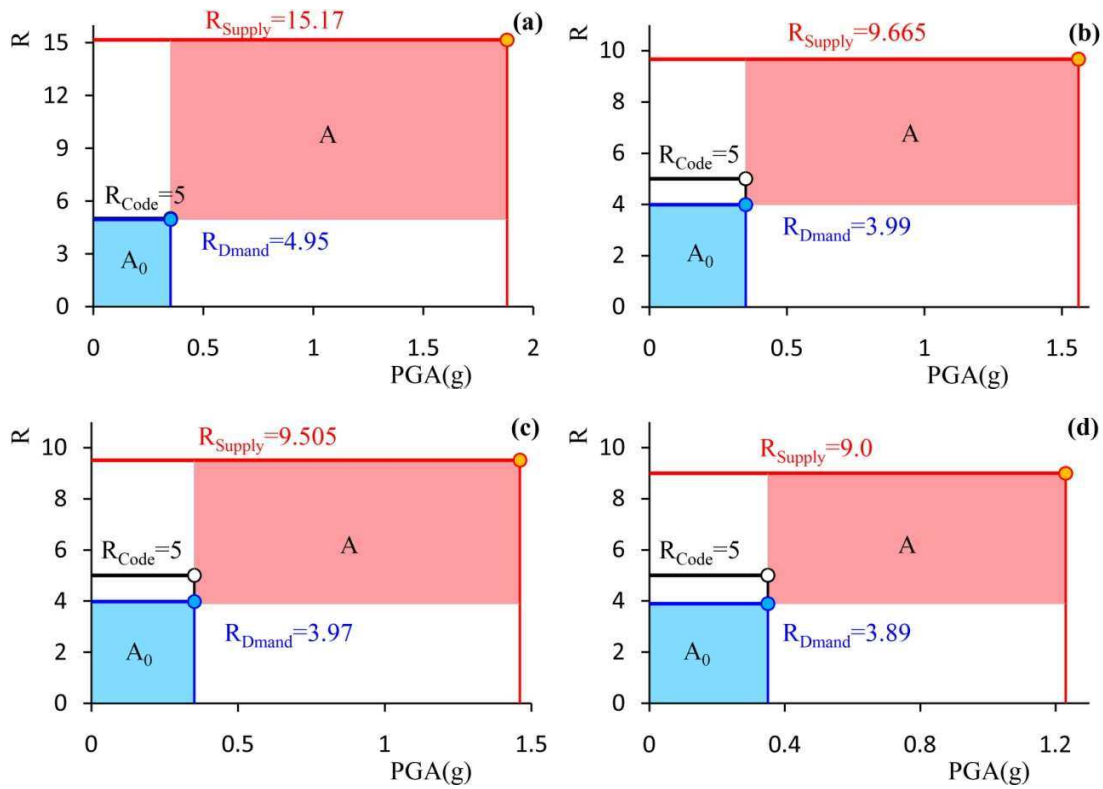
422 For better comparison, Fig (13) demonstrates the effect of building's height on the code-based,
423 demand and supply response modification factors. For each value of response modification factor
424 in the grey zone shown in this figure, the structures are expected to be rated in the performance
425 levels higher than life safety (LS) under the DBE or events with lower intensities. This implies
426 that using code-based R-factor equal to 5 in the preliminary design process can ensure the
427 structural safety and stability of the buildings under DBE hazard level. It can be noted that this
428 value of response modification factor can also guarantee that the structures satisfy the life safety
429 (LS) performance criteria in the event of MCE scenario ($PGA=0.55g$).

430 As it is observed in Fig (13), although increasing the building's height reduces the demand and
431 supply response modification factors, the rate of variations is not significant (except for the 3-
432 storey building). This trend is more profound for the demand response modification factor. The
433 results also indicate that by decreasing the building's height, in general, the safety margin
434 increases. Moreover, parametric analysis of the demand and supply response modification factors
435 shows that as the building's height increases, the modification factors obtained from ductility
436 (R_μ) and over-strength (Ω_s) are respectively improved and reduced. This is most likely due to the
437 shear and rigid behaviour of shorted buildings and flexural and membrane behaviour of the taller
438 ones.

439 It should be noted that, with respect to the considerable redundancy and stiffness of tunnel-form
440 buildings, in most cases (especially when low-rise structures are of concern), the minimum code
441 requirements will govern the design of structural elements. This can lead to oversized sections,
442 which increases the constructional costs of these structures. Therefore, the results suggest that
443 tunnel-form structural system is more suitable for construction of the mid and high-rise building

444 structures. While more studies may be required to develop more accurate response modifications
 445 factors for irregular tunnel-form buildings, the results of this study should prove useful in the
 446 preliminary performance-based design of these systems.

447

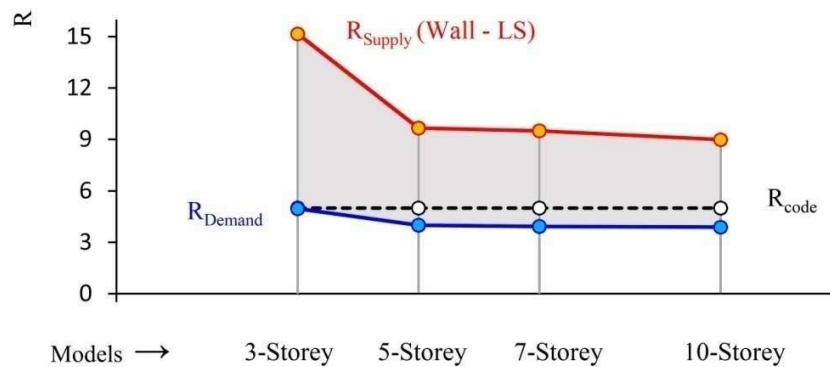


448

449

450 **Fig (12): Code-Based, Demand and Supply Response Modification Factors for (a) 3-storey, (b) 5-storey, (c) 7-**
 451 **storey, and (d) 10- storey buildings**

452



453

454 **Fig (13): Effect of building's height on the Code-Based, Demand and Supply Response Modification Factors**

455

456 Natural Frequencies of Irregular Tunnel-Form Buildings

457 As mentioned before, analysis of the characteristics of the vibration modes of the irregular
458 tunnel-form buildings in this study showed that the translational and torsional displacements in
459 the first mode (along y direction) are coupled (see Table (1)). The results also indicated that
460 torsional displacements in general possess a greater share compared to translation displacements.

461 To assess the torsional stiffness, Ω parameter is defined as the ratio of torsional to translational
462 frequencies of the structure using the following equation:

$$\Omega = \sqrt{\frac{K_{\theta}}{K} \times \frac{M}{I_M}} \quad (7)$$

463 In this equation, K_{θ} , I_M , K and M , respectively denote the torsional stiffness, mass moment of
464 inertia, lateral stiffness and building's mass. In this study, Ω parameter was estimated for all the
465 horizontally irregular structures. Torsional stiffness and mass moment of inertia have been
466 calculated at the centres of rigidity and mass, respectively (Annigeri and Mittal 1996). In this
467 respect, Equation (7) can be rewritten as:

$$\Omega^2 = \frac{K_{\theta,CS} \times M}{I_{M,CM} \times K} = \frac{\rho_K^2}{\rho_M^2} \quad (8)$$

468 where ρ_K and ρ_M represent the scaled stiffness and mass gyration radius about centres of rigidity
469 and mass, which are calculated from equations (9) and (10). It is noted that “b” represents the
470 plan's width.

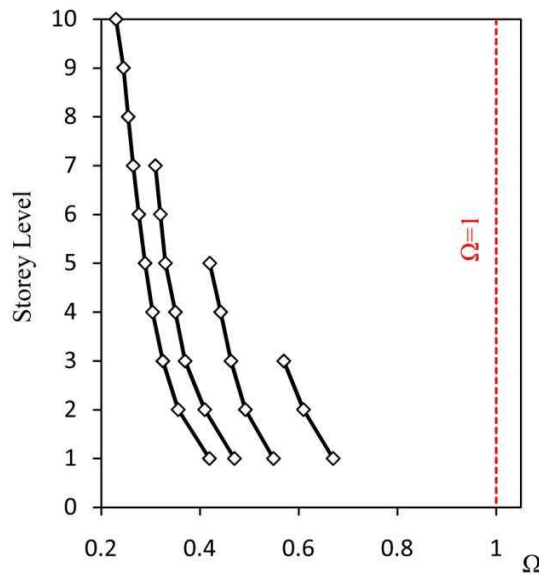
$$\rho_k = \frac{1}{b} \sqrt{\frac{K_{\theta,CS}}{K}}, \quad \rho_m = \frac{1}{b} \sqrt{\frac{I_{M,CS}}{M}} \quad (9), (10)$$

471 It should be mentioned that calculation of the above parameter by using Equations (9) and (10)
472 can be a difficult task. To tackle this issue, in this study the torsional index (Δ) is employed. This
473 index is defined as the ratio of displacements of left and right edges of storey diaphragms while
474 structure is in elastic range of behaviour. It is obtained by conduction pushover analysis, in which
475 loading pattern is triangular and lateral loads are applied to the mass centres. Subsequently, ρ_K is
476 calculated based on Equation (11) as suggested by Tso and Wong (1995).

$$\Delta = \frac{\delta_{\min}}{\delta_{\max}} = 1 - \left(\frac{e}{\rho_k^2} \right) \left(1 + \left(\frac{e}{\rho_k^2} \right) (0.5 + \eta) \right)^{-1} \quad (11)$$

477 where δ_{\min} and δ_{\max} are minimum and maximum displacements of the edge, respectively
 478 (displacement of stiff edge of diaphragm as shown in Fig 1); Δ represents the ratio of minimum
 479 to maximum displacements; and e and η are the distance between centres of rigidity and mass and
 480 the distance between the centres of geometry and rigidity, respectively (both normalized to the
 481 plan's width). In this study, for each storey, ρ_k is calculated based on the latter equation.

482 Fig (14) shows the Ω parameter calculated for each storey of the studied buildings. It is shown
 483 that Ω for all buildings is less than 1, which means the dominant behaviour of the buildings is
 484 governed by torsional displacements. Interestingly, as the number of storeys increases, the value
 485 of this parameter is reduced indicating the fact that torsion is intensified in the upper storeys. In
 486 this regard, smaller Ω values have been calculated for the taller buildings implying the higher
 487 effects of torsion developed in this building. Based on the results, employing the drift at mass
 488 centre cannot accurately represent the distribution of maximum responses developed in the
 489 storeys. Also it is shown that, due to the high torsional movements developed in the upper
 490 storeys, the centre of the roof may not be a proper choice for displacement requirements.
 491 Therefore, to assess the level of damage, it is recommended to use other response parameters
 492 such as flexible edge displacements or the maximum strains in the structural elements.

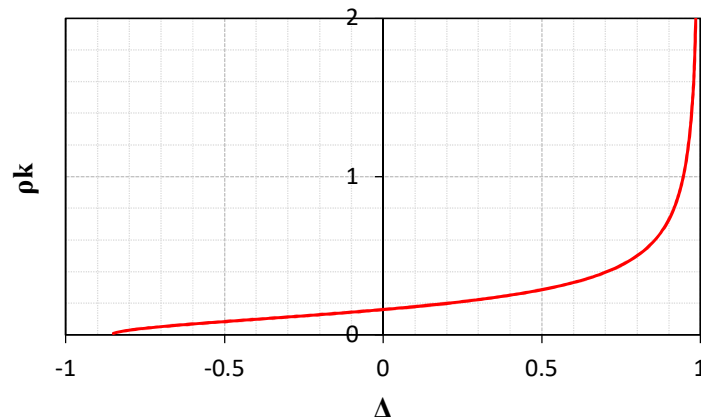


493 Fig (14): Uncoupled frequency ratios for 3, 5, 7 and 10-storey buildings
 494

495 For better insight, Equation (11) can be rewritten in the following form:

496
$$\rho_k^2 = \left(\frac{0.5(1+\Delta)}{1-\Delta} - \eta \right) e \quad (12)$$

497 Fig (15) shows the scaled torsional stiffness (ρ_k) as a function of minimum to maximum
498 displacement ratio (Δ) for the tunnel-form buildings used in this study. In general, it is shown that
499 increasing Δ results in an increase in ρ_k . When the minimum and maximum displacements of the
500 edge are equal and in the same direction (i.e. $\Delta=1$), ρ_k tends to infinity indicating a complete
501 translation displacement. On the contrary, for the case where the minimum and maximum
502 displacements of the edge are equal but in the opposite direction (i.e. $\Delta=-1$), ρ_k tends to zero
503 representing a dominant torsional behaviour.



504
505 **Fig (15): Scaled torsional stiffness (ρ_k) as a function of minimum to maximum displacement ratio (Δ), $e= 0.056$**
506 **and $\eta= 0.039$**

507 **Conclusions**

508 With reference to the models studied herein and the assumptions made, the results indicate that
509 the tunnel-form structural system is capable to exhibit acceptable seismic performance despite the
510 presence of horizontal geometric irregularity. Based on the results obtained, the requirement of
511 being horizontally regular for tunnel-form buildings seems to be too conservative at least for the
512 buildings studied herein.

- 513 1. The earthquake intensity required for the walls and coupling beams to reach various
514 performance levels was estimated to be several times greater than that of DBE hazard
515 level. Therefore, it is reasonable to expect an elastic behaviour from these structures even
516 under strong ground motions.

- 517 2. Based on the probabilistic investigations on 3, 5, 7 and 10-storey tunnel-form irregular
518 buildings, the probability for the coupling beams to reach the performance level of
519 immediate occupancy (IO) is less than 2 and 19% under DBE and MCE hazard levels,
520 respectively. Likewise, the probability of reaching the same performance level for the
521 walls is approximately 0 and 2%, respectively. This indicates that the studied buildings
522 can practically satisfy IO performance level under both hazard levels.
- 523 3. Due to the larger seismic demands of coupling beams compared to those of the walls,
524 these elements can act as a seismic fuse in tunnel-form buildings to absorb and dissipate
525 the earthquake input energy, especially in lower seismic intensities
- 526 4. For a specific level of intensity, the seismic reliability of tunnel-form buildings is
527 generally reduced as the height (i.e. number of storeys) increases. This trend is especially
528 evident in the case of coupling beams.
- 529 5. The governing behaviour of the horizontally irregular tunnel-form buildings studied
530 herein is a flexible torsional mode, in which the torsional response is intensified by
531 increasing in the building's height. Besides, it was found that, in general, the diaphragm
532 rotational displacements increase from the bottom to the top of the structures. Irregularity-
533 induced torsions also intensify the displacement demands in the perimeter parts of the
534 buildings and thus, damages are initiated from those parts.
- 535 6. With respect to the greater values of displacement raised by torsion compared to the
536 translational movements, it appears that using the drift at storey mass centre as damage
537 measure (DM) is not appropriate for irregular tunnel-form buildings. In this respect, other
538 damage measures such as flexible edge drift or local damage measures for beams and
539 walls are recommended.
- 540 7. Response modification factor of the studied buildings based on the selected hazard levels
541 is smaller than the values estimated for the supply modification factor when the walls
542 reach the life safety performance level. This highlights the fact that such structures exhibit
543 sufficient strength and safety under intense hazard levels. It was shown that considering
544 the code-based response modification factor of 5 for preliminary design of irregular
545 tunnel-form buildings can ensure the structural safety and stability of the buildings under
546 both DBE and MCE hazard scenarios.

547 8. Parametric analysis on the demand and supply response modification factors indicates
548 that increasing the building's height results in an increase and a decrease in the
549 modification factors originated by ductility and over-strength, respectively. Increasing the
550 building's height, can also transform the shear-dominant behaviour to the membrane and
551 flexural type response in tunnel-form structural systems.

552

553 **References**

- 554 ACI Committee 318 (2014). Building code requirements for structural concrete (ACI 318-14)
555 and commentary, American Concrete Institute.
- 556 Allouzi R, Alkloub A (2017) New nonlinear dynamic response model of squat/-slender
557 flanged/non-flanged reinforced concrete walls, *Structural Concrete*, PP.1-15.
- 558 Ang AHS, Tang WH (2007) *Probability Concepts in Engineering: Emphasis on Applications to*
559 *Civil and Environmental Engineering*, 1, Wiley, 2nd Edition, the University of Michigan.
- 560 Annigeri S, Mittal AK (1996) Uncoupled Frequency Ratio in Asymmetric Buildings, *Earthquake*
561 *Engineering and Structural Dynamics*, 25, PP.871-881.
- 562 ASCE (2014) Seismic rehabilitation of existing buildings, ASCE/SEI41-13, American Society of
563 Civil Engineers.
- 564 ASCE (2016) Minimum Design Loads and Associated Criteria for Buildings and Other
565 Structures, ASCE/SEI 7-16, American Society of Civil Engineers, Reston, Virginia.
- 566 ATC (1995) Structural Response Modification Factors, ATC-19 Report, Applied Technology
567 Council, Redwood City, California.
- 568 ATC (1996), Seismic Evaluation of Concrete Buildings, Vol.1, ATC-40, Applied Technology
569 Council, Redwood, CA.
- 570 Balkaya C, Kalkan E (2003a) Estimation of fundamental periods of shear-wall dominant building
571 structures, *Earthquake Engineering and structural dynamics*, 32(7), PP. 985-998.
- 572 Balkaya C, Kalkan E (2003b) Seismic Design Parameters for Shear-Wall Dominant Building
573 Structures, 14th national congress on Earthquake Engineering, Mexico.
- 574 Balkaya C, Kalkan E (2004b) Seismic Vulnerability, Behavior and Design of Tunnel Form
575 Building Structures, *Engineering Structures*, 26(14), PP.2081-2099.
- 576 Balkaya C, Yuksel SB, Derinoz O (2012) Soil-Structure Interaction Effects on the Fundamental
577 Periods of the Shear-Wall Dominant Buildings, *The Structural Design of Tall and Special*
578 *Buildings*, 21(6), PP.416-430.
- 579 Balkaya, C., Kalkan, E. (2004a) Relevance of R-Factor and Fundamental Period for Seismic
580 Design of Tunnel-Form Building, 13th World Conference on Earthquake Engineering,
581 Vancouver, Canada.
- 582 Beheshti-Aval SB, Mohsenian V, Sadegh-Kouhestani H (2018) Seismic performance-based
583 assessment of tunnel form buildings subjected to near- and far-fault ground motions, *Asian*
584 *Journal of Civil Engineering*, 19(1), PP.79-92.

585 Berahman F, Behnamfar F (2007) Seismic Fragility Curves for Un Anchored on-Grade Steel
586 Storage Tanks: Bayesian Approach, *Journal of Earthquake Engineering*, 11, PP.166-192.

587 BHRCF (2007) Approved technologies indirection of sub-note 2-6, paragraph "D", Note
588 6, "A step in direction of building industrialization", first edition, Building and Housing
589 Research Center Press, pages 21 and 22.

590 CEN (Comité Européen de Normalization) (2004). Eurocode 8: Design of structures for
591 earthquake resistance-Part 1: General rules, seismic actions and rules for buildings, EN 1998-
592 1-1, Brussels.

593 Cimellaro GP, Reinhorn AM, Bruneau M, Rutenberg A (2006) Multi-Dimensional Fragility of
594 Structures: Formulation and Evaluation, Technical Report MCEER-06-0002.

595 Computers and Structures Inc. (CSI), (2015). Structural and Earthquake Engineering Software,
596 ETABS, Extended Three Dimensional Analysis of Building Systems Nonlinear Version
597 15.2.2, Berkeley, CA, USA.

598 Computers and Structures Inc. (CSI), (2016), Structural and Earthquake Engineering Software,
599 PERFORM-3D Nonlinear Analysis and Performance Assessment for 3D Structures, Version
600 6.0.0, Berkeley, CA, USA.

601 Fajfar P (2000) A Nonlinear Analysis Method for Performance Based Seismic Design,
602 *Earthquake Spectra*, 116 (3), PP.573-592.

603 Fanaie N, AfsarDizaj E (2014) Response modification factor of the frames braced with reduced
604 yielding segment BRB, *Structural Engineering and Mechanics*, 50(1), PP. 1-17.

605 Ghobarah A (2004). On drift limits associated with different damage levels. International
606 Workshop on Performance-based Seismic Design Concepts and Implementation, Bled,
607 Slovenia.

608 Goel RK, Chopra AK (1998) Period Formulas for Concrete Shear Wall Buildings, *Journal of*
609 *Structural Engineering*, 124(4), PP.426-433.

610 Hajirasouliha I, Pilakoutas K, Mohammadi RK (2016) Effects of uncertainties on seismic
611 behaviour of optimum designed braced steel frames. *Steel and Composite Structures*, 20(2),
612 pp. 317-335.

613 Hancock J, Watson-Lamprey J, Abrahamson NA, Bommer JJ, Markatis A, McCoy E, Mendis R
614 (2006) An Improved Method of Matching Response Spectra of Recorded Earthquake Ground
615 Motion Using Wavelets, *Journal of Earthquake Engineering*, 10,PP. 67-89.

616 Kalkan E, Yuksel SB (2007) Pros and Cons of Multi Story RC Tunnel-Form (Box-Type)
617 Buildings, *The Structural Design of Tall and Special Buildings*, 17(3), PP.601-617.

618 Kinali K (2007) Seismic Fragility Assessment of Steel Frames in the Central and Eastern United
619 States, APh.D Thesis, School of Civil and Environmental Engineering, Georgia Institute of
620 Technology.

621 Klasanovic I, Kraus I, Hadzima-Nyarko Ma (2014) Dynamic Properties of Multistory Reinforced
622 Concrete Tunnel-Form Building – A Case Study in Osijek, Croatia, *Forecast Engineering:*
623 *Global Climate change and the challenge for built environment*, Weimar, Germany.

624 Lee L, Chang K, Chun Y (2000) Experimental Formula for the Fundamental Period of RC
625 Building with Shear Wall Dominant Systems, *Structural Design of Tall Buildings*, 9(4), PP.
626 295-307.

627 Lia SP, Biggs JM (1980) Inelastic response spectra for seismic building design, Journal of the
628 Structural Division (ASCE) 106(ST6), PP.1295-1310.

629 Miranda E (1991) Seismic evaluation & upgrading of existing buildings, A P.hd Thesis,
630 University of California @ Berkeley.

631 Mohsenian V, Mortezaei A (2018a) Seismic reliability evaluation of tunnel form (box-type) RC
632 structures under the accidental torsion, Structural Concrete, pp.1-12, DOI:
633 10.1002/suco.201700276.

634 Mohsenian V, Mortezaei A (2018b), Effect of steel coupling beam on the seismic reliability
635 and *R*-factor of box-type buildings, Structures and Buildings.

636 Mwafy AM, Elnashai AS (2002) Calibration of force reduction factors of RC buildings. Journal
637 of Earthquake Engineering, 6(2), PP. 239-273.

638 Nielson BG (2005) Analytical Fragility Curves for Highway Bridges in Moderate Seismic Zones,
639 A Ph.D Thesis, School of Civil and Environmental Engineering, Georgia Institute of
640 Technology.

641 Paulay T, Binney JR (1974) Diagonally reinforced coupling beams of shear walls”, Shear in
642 reinforced concrete, ACI Special Publications 42, PP.579-598.

643 PEER Ground Motion Database, Pacific Earthquake Engineering Research Center, Web Site:
644 http://peer.berkeley.edu/peer_ground_motion_database.

645 Permanent Committee for Revising the Standard 2800, Iranian Code of Practice for Seismic
646 Resistant Design of Buildings, 4th Edition, Building and Housing Research Center, 2014,
647 Tehran, Iran.

648 Shome N, Cornell CA (1999) Probabilistic Seismic Demand Analysis of Nonlinear Structures,
649 Reliability of Marine Structures Report No: RMS-35, Civil and Environmental Engineering,
650 Stanford University.

651 Tavafoghi A, Eshghi S (2008) Seismic Behavior of Tunnel Form Concrete Building Structures,
652 14th World Conference on Earthquake Engineering, 12-17 October, Beijing, China.

653 Tavafoghi A, Eshghi S (2011) Evaluation of behavior factor of tunnel-form concrete building
654 structures using Applied Technology Council 63, The Structural Design of Tall and Special
655 Buildings, 22(8), PP.615-634.

656 Tso WK, Wong CM (1995) Eurocode8 seismic torsional provision evaluation, European
657 Earthquake Engineering, IX, 9(1), PP.23-33.

658 Vamvatsikos D, Cornell CA (2002) Incremental Dynamic Analysis, Earthquake Engineering
659 Structural Dynamics, 31(3), PP.491-514.

660 Whittaker A, Hart G, Rojahn C (1999) Seismic response modification factors, Journal of
661 Structural Engineering, 125, PP. 438-444.

662 Yuksel SB, Kalkan E (2007) Behavior of Tunnel form Buildings under quasi_static cyclic lateral
663 loading, Structural Engineering and Mechanics, 27(1), PP.99-115.

664 Zhao ZZ, Kwan AKH, He XG (2004) Nonlinear Finite Element Analysis of Deep Reinforced
665 Concrete Coupling Beams, Engineering Structures, 26(1), PP.13-25.